
On Unifying Deep Generative Models

Zhiting Hu^{1,2} Zichao Yang¹ Ruslan Salakhutdinov¹ Eric P. Xing^{1,2}
Carnegie Mellon University¹, Petuum Inc.²

Abstract

Deep generative models have achieved impressive success in recent years. Generative Adversarial Networks (GANs) and Variational Autoencoders (VAEs), as powerful frameworks for deep generative model learning, have largely been considered as two distinct paradigms and received extensive independent study respectively. This paper establishes formal connections between deep generative modeling approaches through a new formulation of GANs and VAEs. We show that GANs and VAEs are essentially minimizing KL divergences of respective posterior and inference distributions with opposite directions, extending the two learning phases of classic wake-sleep algorithm, respectively. The unified view provides a powerful tool to analyze a diverse set of existing model variants, and enables to exchange ideas across research lines in a principled way. For example, we transfer the importance weighting method in VAE literatures for improved GAN learning, and enhance VAEs with an adversarial mechanism for leveraging generated samples. Quantitative experiments show generality and effectiveness of the imported extensions.

1 Introduction

Deep generative models define distributions over a set of variables organized in multiple layers. Early forms of the deep generative models dated back to works on hierarchical Bayesian models [40] and neural network models such as the Helmholtz machines [11], originally studied in the context of unsupervised learning, latent space modeling, etc. Such models are usually trained via an EM style framework, using either a variational inference [27] or a data augmentation [12, 53] algorithm. Of particular relevance to this paper is the classic wake-sleep algorithm dates by Hinton et al. [21] for training Helmholtz machines, as it explored an idea of minimizing a pair of KL divergences in opposite directions of the posterior and its approximation, and the predictability minimization algorithm by Schmidhuber [51] which presented the early form of adversarial approaches.

In recent years there has been a resurgence of interests in deep generative modeling. The emerging approaches, including Variational Autoencoders (VAEs) [28], Generative Adversarial Networks (GANs) [16], Generative Moment Matching Networks (GMMNs) [33, 13], auto-regressive neural networks [31, 43], and so forth, have led to impressive results in a myriad of applications, such as image and text generation [48, 25, 34, 55], disentangled representation learning [8, 30], and semi-supervised learning [50, 29].

The deep generative model literature has largely viewed these approaches as distinct model training paradigms. For instance, GANs aim to achieve an equilibrium between a generator and a discriminator; while VAEs are devoted to maximizing a lower bound of the data log-likelihood. A rich array of theoretical analyses and model extensions have been developed independently for GANs [1, 2, 50, 41] and VAEs [5, 10, 25, 17], respectively. A few works attempt to combine the two objectives in a single model for improved inference and sample generation [32, 35, 52, 54]. Despite the significant progress specific to each method, it remains unclear how these apparently divergent approaches connect to each other in a principled way.

In this paper, we present a new formulation for deep generative models that connects the GANs and VAEs under a unified view, and links them back to the classic wake-sleep algorithm. We show that GANs and VAEs are in fact minimizing opposite KL divergences of respective posterior and inference distributions, and extending the sleep and wake phases, respectively, for generative model learning. More specifically, we develop a Bayesian reformulation of GANs that interprets generation of samples as performing posterior inference, leading to an objective that resembles variational inference as in VAEs. As a counterpart, VAEs in our interpretation contain a degenerated adversarial mechanism that blocks out generated samples from contributing to model training.

The proposed interpretation provides a useful tool to analyze the broad class of recent GAN- and VAE-based algorithms, enabling perhaps a more principled and unified view of the landscape of generative modeling. For instance, one can easily extend our formulation to subsume InfoGAN [8] that additionally infers hidden representations of examples, VAE/GAN joint models [32, 6] that offer improved generation and reduced mode missing, and adversarial domain adaptation (ADA) [15, 46, 47, 9] that is traditionally framed in the discriminative setting.

The close parallelisms between GANs and VAEs further ease mutual exchange of ideas that were originally proposed separately for improving each individual class of models, to in turn benefit the other class. We provide two examples in such spirit in this paper: 1) Drawn inspiration from importance weighted VAE (IWAE) [5], we straightforwardly derive importance weighted GAN (IWGAN) that maximizes a tighter lower bound on the marginal likelihood compared to the vanilla GAN. 2) Motivated by the GAN adversarial game we activate the originally degenerated discriminator in VAEs, resulting in a full-fledged model that adaptively leverages both real and fake examples. Our quantitative empirical results show that the techniques imported from the other class are generally applicable to the base model and its variants, yielding consistently better performance.

2 Related Work

There has been a surge of research interest in deep generative models in recent years, with remarkable progress made in understanding several class of algorithms. The wake-sleep algorithm [21] is one of the earliest general approaches for learning deep generative models. The algorithm incorporates a separate inference model for posterior approximation, and aims at maximizing a variational lower bound of the data log-likelihood, or equivalently, minimizing the KL divergence of the approximate posterior and the true posterior. However, besides the wake phase that minimizes the KL divergence w.r.t the generative model, the sleep phase is introduced for tractability that minimizes instead the *reversed* KL divergence w.r.t the inference model. Recent approaches such as Neural Variational Inference and Learning (NVIL) [38] and Variational Autoencoders (VAEs) [28] are developed to maximize the variational lower bound w.r.t both the generative and inference models jointly. To reduce the variance of stochastic gradient estimates for inference model updates, NVIL incorporates control variates [44] as in the reinforcement learning literature [56], while VAEs leverage reparametrized gradients. Many works have been done along the line of improving VAEs. Burda et al. [5] develop importance weighted VAEs to obtain a tighter lower bound. Goyal et al. [17] enable complex latent code space with Bayesian nonparametric priors. As VAEs do not involve a sleep phase-like procedure, generated samples from the generative model are not leveraged for model learning. Hu et al. [25] combine VAEs with an extended sleep procedure that exploits generated samples for learning.

Another emerging family of deep generative models is the Generative Adversarial Networks (GANs) [16], in which a discriminator is trained to distinguish between real and generated samples and the generative model is trained to confuse the discriminator. The adversarial approach can be alternatively motivated in the perspectives of approximate Bayesian computation [18] and density ratio estimation [39]. The original objective of the generator is to minimize the log probability of the discriminator correctly recognizing a generated sample as fake. This is equivalent to *minimizing a lower bound* on the Jensen-Shannon divergence (JSD) of the generator distribution and data distribution [16, 41]. Besides, the objective suffers from vanishing gradient issue when the discriminator is too strong, and in practice people have used another objective which maximizes the log probability of the discriminator recognizing a generated sample as real [16, 41, 1]. The second objective has the same optimal solution as with the original one. We base our analysis of GANs on the second objective as it is widely used in practice. Previous study of GANs has largely assume optimal discriminator, which, as show in [2], can have exponentially high VC dimension. Our formulation avoids the optimality assumption, yielding results close to the practice. Numerous extensions of

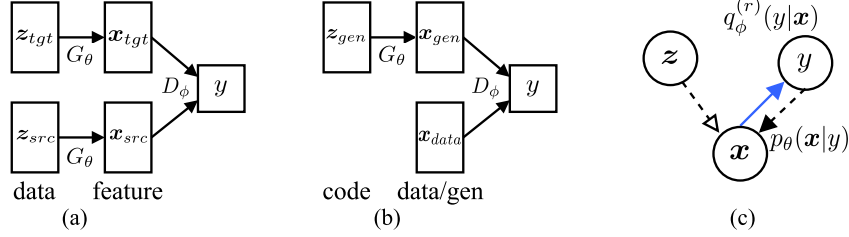


Figure 1: **(a)** Conventional view of ADA: from source domain (src) to target domain (tgt); **(b)** Conventional view of GAN: the code space of real data is degenerated; **(c)** Graphical model of both ADA and GAN (Eq.3). Arrows with solid lines denote generative process; arrows with dashed lines denote inference; hollow arrows denote deterministic transformation leading to implicit distributions; and blue arrows denote adversarial mechanism that involves respective conditional p and its reversed distribution p^r , e.g., $q(y|x)$ and $q^r(y|x)$ in ADA and GANs (denoted as $q^{(r)}(y|x)$ for short). For clarity we also label the respective conditional distributions of each node. Prior distributions are omitted. In GANs we interpret generating samples x as performing inference. See the text for more details.

GANs have been developed, including combination of VAEs for improved generation [32, 35, 6], and generalization of the objectives to minimize other f-divergence criteria beyond JSD [41, 52]. The adversarial principle has gone beyond the generation setting and been applied to other contexts such as domain adaptation [15, 47, 46, 9], and Bayesian inference [36, 54, 26, 49] which uses implicit variational distributions in VAEs and leverage the adversarial approach for optimization. This paper starts from the basic models of GANs and VAEs, and develops a general formulation that reveals underlying connections of different classes of approaches and easily extends to many of the above variants, yielding a unified view of the broad set of deep generative modeling.

3 Bridging the Gap

The wake sleep algorithm trains a generative model jointly with an inference model. The sleep phase updates the inference model with the samples from the generator, and the wake phase updates the generator by reconstructing data conditioned on latent code from the inference model. In GANs, the generative model is trained by passing generated samples to a discriminator and minimizing the resulting error evaluated by the discriminator. Intuitively, the reliance on fake samples for learning resembles the sleep phase in the wake-sleep algorithm. In contrast, VAEs train the generative model by reconstructing observed real examples, sharing similarity to the wake phase. This section formally explores these connections.

For ease of presentation and to establish a systematic notation for the paper, we start with a new interpretation of *Adversarial Domain Adaptation* (ADA) [15] within our proposed formulation. We then show that GANs are a special case of ADA with a degenerated source domain, and reveal close relations to VAEs and wake-sleep algorithm through KL divergence interpretation of the objectives.

3.1 Adversarial Domain Adaptation (ADA)

ADA aims to transfer prediction knowledge learned from a source domain with labeled data to a target domain without labels, by learning domain-invariant features [15, 47, 46, 9]. That is, it learns a feature extractor whose output cannot be distinguished by a discriminator between the source and target domains.

We first review the conventional formulation of ADA. Figure 1(a) illustrates the computation flow of the algorithm. Let z be a data example either in the source or target domain, and $y \in \{0, 1\}$ the domain indicator with $y = 0$ indicating the target domain and $y = 1$ the source domain. The data distributions conditioning on the domain are then denoted as $p(z|y)$. The feature extractor G_θ parameterized with θ maps z to feature $x = G_\theta(z)$. To enforce domain invariance of feature x , a discriminator D_ϕ is learned to adversarially distinguish between the two domains. That is, $D_\phi(x)$ outputs the probability that x comes from the source domain, and the discriminator is trained to

maximize the binary classification accuracy of recognizing the feature domains:

$$\max_{\phi} \mathcal{L}_{\phi} = \mathbb{E}_{\mathbf{x}=G_{\theta}(\mathbf{z}), \mathbf{z} \sim p(\mathbf{z}|y=1)} [\log D_{\phi}(\mathbf{x})] + \mathbb{E}_{\mathbf{x}=G_{\theta}(\mathbf{z}), \mathbf{z} \sim p(\mathbf{z}|y=0)} [\log(1 - D_{\phi}(\mathbf{x}))]. \quad (1)$$

The feature extractor G_{θ} is then trained to fool the discriminator:

$$\max_{\theta} \mathcal{L}_{\theta} = \mathbb{E}_{\mathbf{x}=G_{\theta}(\mathbf{z}), \mathbf{z} \sim p(\mathbf{z}|y=1)} [\log(1 - D_{\phi}(\mathbf{x}))] + \mathbb{E}_{\mathbf{x}=G_{\theta}(\mathbf{z}), \mathbf{z} \sim p(\mathbf{z}|y=0)} [\log D_{\phi}(\mathbf{x})]. \quad (2)$$

Here we omit the additional loss on θ that fits the features to the data label pairs of source domain (see the supplementary materials for the details).

With the background of the conventional formulation, we now frame our new interpretation of ADA. The data distribution $p(\mathbf{z}|y)$ and deterministic transformation G_{θ} together form an *implicit* distribution over \mathbf{x} , denoted as $p_{\theta}(\mathbf{x}|y)$, which is intractable to evaluate likelihood but easy to sample from. Let $p(y)$ be the prior distribution of the domain indicator y , e.g., a uniform distribution as in Eqs.(1)-(2). The discriminator defines a conditional distribution $q_{\phi}(y|\mathbf{x}) = D_{\phi}(\mathbf{x})$. Let $q_{\phi}^r(y|\mathbf{x}) = q_{\phi}(1 - y|\mathbf{x})$ be the reversed distribution over domains. The objectives of ADA are therefore rewritten as (omitting the constant scale factor 2):

$$\begin{aligned} \max_{\phi} \mathcal{L}_{\phi} &= \mathbb{E}_{p_{\theta}(\mathbf{x}|y)p(y)} [\log q_{\phi}(y|\mathbf{x})] \\ \max_{\theta} \mathcal{L}_{\theta} &= \mathbb{E}_{p_{\theta}(\mathbf{x}|y)p(y)} [\log q_{\phi}^r(y|\mathbf{x})]. \end{aligned} \quad (3)$$

The above objectives can be interpreted as maximizing the log likelihood of y (or $1 - y$) with the “generative distribution” $q_{\phi}(y|\mathbf{x})$ conditioning on the latent code \mathbf{x} inferred by $p_{\theta}(\mathbf{x}|y)$. Note that the *only* (but critical) difference of the objectives of θ from ϕ is the replacement of $q(y|\mathbf{x})$ with $q^r(y|\mathbf{x})$. This is where the adversarial mechanism comes about.

Graphical model representation Figure 1(c) illustrates the graphical model of the formulation in Eq.(3), where, in the new view, solid-line arrows denote the *generative process* while dashed-line arrows denote the *inference process*. We introduce new visual elements, e.g., hollow arrows for expressing implicit distributions, and blue arrows for adversarial mechanism. As noted above, adversarial modeling is achieved by swapping between $q(y|\mathbf{x})$ and $q^r(y|\mathbf{x})$ when training respective modules.

3.2 Generative Adversarial Networks (GANs)

GANs [16] can be seen as a special case of ADA. Taking image generation for example, intuitively, we want to transfer the properties of the source domain (real images) to the target domain (generated images), making them indistinguishable to the discriminator. Figure 1(b) shows the conventional view of GANs.

Formally, \mathbf{x} now denotes a real example or a generated sample, \mathbf{z} is the respective latent code. For the generated sample domain ($y = 0$), the implicit distribution $p_{\theta}(\mathbf{x}|y = 0)$ is defined by the prior of \mathbf{z} and the generator $G_{\theta}(\mathbf{z})$, which is also denoted as $p_{g_{\theta}}(\mathbf{x})$ in the literature. For the real example domain ($y = 1$), the code space and generator are degenerated, and we are directly presented with a fixed distribution $p(\mathbf{x}|y = 1)$, which is just the real data distribution $p_{data}(\mathbf{x})$. Note that $p_{data}(\mathbf{x})$ is also an implicit distribution allowing efficient empirical sampling. In summary, the distribution over \mathbf{x} is constructed as

$$p_{\theta}(\mathbf{x}|y) = \begin{cases} p_{g_{\theta}}(\mathbf{x}) & y = 0 \\ p_{data}(\mathbf{x}) & y = 1. \end{cases} \quad (4)$$

Here, free parameters θ are only associated with $p_{g_{\theta}}(\mathbf{x})$ of the generated sample domain, while $p_{data}(\mathbf{x})$ is constant. As in ADA, discriminator D_{ϕ} is simultaneously trained to infer the probability that \mathbf{x} comes from the real data domain. That is, $q_{\phi}(y = 1|\mathbf{x}) = D_{\phi}(\mathbf{x})$.

With the established correspondence between GANs and ADA, we can see that the objectives of GANs are precisely expressed as Eq.(3) and as the graphical model in Figure 1(c). To make this clearer, we recover the classical form by unfolding over y and plugging in conventional notations. For instance, the objective of the generative parameters θ is translated into

$$\begin{aligned} \max_{\theta} \mathcal{L}_{\theta} &= \mathbb{E}_{p_{\theta}(\mathbf{x}|y=0)p(y=0)} [\log q_{\phi}^r(y = 0|\mathbf{x})] + \mathbb{E}_{p_{\theta}(\mathbf{x}|y=1)p(y=1)} [\log q_{\phi}^r(y = 1|\mathbf{x})] \\ &= \frac{1}{2} \mathbb{E}_{\mathbf{x}=G_{\theta}(\mathbf{z}), \mathbf{z} \sim p(\mathbf{z}|y=0)} [\log D_{\phi}(\mathbf{x})] + \frac{1}{2} \mathbb{E}_{\mathbf{x} \sim p_{data}(\mathbf{x})} [\log(1 - D_{\phi}(\mathbf{x}))] \\ &= \frac{1}{2} \mathbb{E}_{\mathbf{x}=G_{\theta}(\mathbf{z}), \mathbf{z} \sim p(\mathbf{z}|y=0)} [\log D_{\phi}(\mathbf{x})] + const, \end{aligned} \quad (5)$$

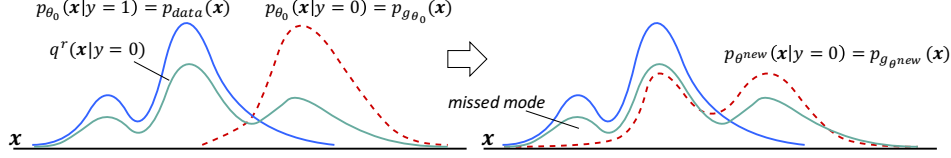


Figure 2: One optimization step of the parameter θ through Eq.(6) at point θ_0 . The posterior $q^r(\mathbf{x}|y)$ is a mixture of $p_{\theta_0}(\mathbf{x}|y=0)$ (blue) and $p_{\theta_0}(\mathbf{x}|y=1)$ (red in the left panel) with the mixing weights induced from $q^r_{\phi_0}(y|\mathbf{x})$. Minimizing the KL divergence of Eq.(6) w.r.t θ drives $p_{\theta}(\mathbf{x}|y=0)$ towards the respective mixture $q^r(\mathbf{x}|y=0)$ (green), resulting in a new state where $p_{\theta^{new}}(\mathbf{x}|y=0) = p_{g_{\theta^{new}}}(\mathbf{x})$ gets closer to $p_{\theta_0}(\mathbf{x}|y=1) = p_{data}(\mathbf{x})$. Due to the asymmetry of KL divergence, $p_{g_{\theta^{new}}}(\mathbf{x})$ missed the smaller mode of the mixture $q^r(\mathbf{x}|y=0)$ which is a mode of $p_{data}(\mathbf{x})$.

where the prior $p(y)$ is uniform as is widely set, resulting in the constant scale factor $1/2$. Note that here the generator is trained using the unsaturated objective [16] which is commonly used in practice.

We now take a closer look at the form of Eq.(3) which is essentially reconstructing the real/fake indicator y (or its reverse $1-y$) conditioned on \mathbf{x} . Further, for each optimization step of $p_{\theta}(\mathbf{x}|y)$ at point (θ_0, ϕ_0) in the parameter space, we have

Lemma 1. Let $p(y)$ be the uniform distribution. Let $p_{\theta_0}(\mathbf{x}) = \mathbb{E}_{p(y)}[p_{\theta_0}(\mathbf{x}|y)]$, and $q^r(\mathbf{x}|y) \propto q^r_{\phi_0}(y|\mathbf{x})p_{\theta_0}(\mathbf{x})$. Therefore, the updates of θ at θ_0 have

$$\begin{aligned} \nabla_{\theta} \left[-\mathbb{E}_{p_{\theta}(\mathbf{x}|y)p(y)} [\log q^r_{\phi_0}(y|\mathbf{x})] \right] \Big|_{\theta=\theta_0} = \\ \nabla_{\theta} \left[\mathbb{E}_{p(y)} [KL(p_{\theta}(\mathbf{x}|y) \| q^r(\mathbf{x}|y))] - JSD(p_{\theta}(\mathbf{x}|y=0) \| p_{\theta}(\mathbf{x}|y=1)) \right] \Big|_{\theta=\theta_0}, \end{aligned} \quad (6)$$

where $KL(\cdot \| \cdot)$ and $JSD(\cdot \| \cdot)$ are the KL and Jensen-Shannon Divergences, respectively.

We provide the proof in the supplement materials. Eq.(6) offers several insights into the generator learning in GANs.

- **Resemblance to variational inference.** If we treat y as visible and \mathbf{x} as latent (as in ADA), it is straightforward to see the connections to the variational inference algorithm where $q^r(\mathbf{x}|y)$ plays the role of the posterior, $p_{\theta_0}(\mathbf{x})$ the prior, and $p_{\theta}(\mathbf{x}|y)$ the variational distribution that approximates the posterior. Optimizing the generator G_{θ} is equivalent to minimizing the KL divergence between the variational distribution and the posterior, minus a JSD between the distributions $p_{g_{\theta}}(\mathbf{x})$ and $p_{data}(\mathbf{x})$. The Bayesian interpretation further reveals the connections to VAEs, as we discuss in the next section.
- **Training dynamics.** By definition, $p_{\theta_0}(\mathbf{x}) = (p_{g_{\theta_0}}(\mathbf{x}) + p_{data}(\mathbf{x}))/2$ is a mixture of $p_{g_{\theta_0}}(\mathbf{x})$ and $p_{data}(\mathbf{x})$ with uniform mixing weights, so the “posterior” $q^r(\mathbf{x}|y) \propto q^r_{\phi_0}(y|\mathbf{x})p_{\theta_0}(\mathbf{x})$ is also a mixture of $p_{g_{\theta_0}}(\mathbf{x})$ and $p_{data}(\mathbf{x})$ with mixing weights induced from the discriminator $q^r_{\phi_0}(y|\mathbf{x})$. For the KL divergence to minimize, the component with $y=1$ is $KL(p_{\theta}(\mathbf{x}|y=1) \| q^r(\mathbf{x}|y=1)) = KL(p_{data}(\mathbf{x}) \| q^r(\mathbf{x}|y=1))$ which is a constant. The active component for optimization is with $y=0$, i.e., $KL(p_{\theta}(\mathbf{x}|y=0) \| q^r(\mathbf{x}|y=0)) = KL(p_{g_{\theta}}(\mathbf{x}) \| q^r(\mathbf{x}|y=0))$. Thus, minimizing the KL divergence in effect drives $p_{g_{\theta}}(\mathbf{x})$ to a mixture of $p_{g_{\theta_0}}(\mathbf{x})$ and $p_{data}(\mathbf{x})$. Since $p_{data}(\mathbf{x})$ is fixed, $p_{g_{\theta}}(\mathbf{x})$ gets closer to $p_{data}(\mathbf{x})$. Figure 2 illustrates the training dynamics schematically.
- **Reasons of the missing mode issue.** The negative JSD term is due to the introduction of the “prior” $p_{\theta_0}(\mathbf{x})$ at current point θ_0 . As JSD is symmetric, the missing mode phenomena widely observed in GAN generator [37, 6] is explained by the asymmetry of the KL divergence which tends to concentrate $p_{\theta}(\mathbf{x}|y)$ to large modes of $q^r(\mathbf{x}|y)$ and ignore smaller ones. See Figure 2 for the example.
- **Optimality assumption of the discriminator.** Previous theoretical works have typically assumed (near) optimal discriminator [16, 1]:

$$q_{\phi_0}(y|\mathbf{x}) \approx \frac{p_{\theta_0}(\mathbf{x}|y=1)}{p_{\theta_0}(\mathbf{x}|y=0) + p_{\theta_0}(\mathbf{x}|y=1)} = \frac{p_{data}(\mathbf{x})}{p_{g_{\theta_0}}(\mathbf{x}) + p_{data}(\mathbf{x})}, \quad (7)$$

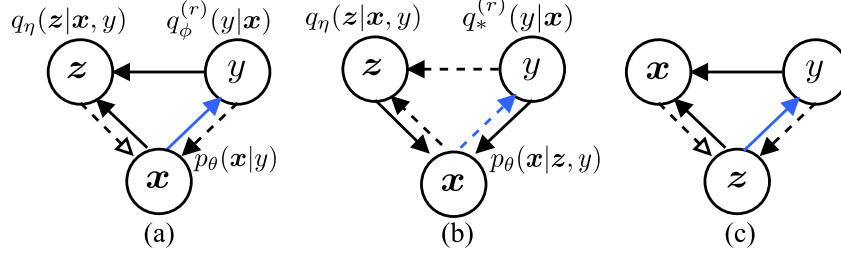


Figure 3: **(a)** Graphical model of InfoGAN (Eq.9), which, compared to GANs (Figure 1(c)), adds conditional generation of code z with distribution $q_\eta(z|x, y)$. See the captions of Figure 1 for the meaning of different types of arrows. **(b)** VAEs (Eq.12), which is obtained by swapping the generation and inference processes of InfoGAN, i.e., in terms of the graphical model, swapping solid-line arrows (generative process) and dashed-line arrows (inference) of (a). **(c)** Adversarial Autoencoder (AAE), which is obtained by swapping data x and code z in InfoGAN (see the supplements for more details).

which can be unwarranted in practice due to limited expressiveness of the discriminator [2]. In contrast, our result does not rely on the optimality assumptions. Indeed, our result is an generalization of the previous theorem [1]: plugging Eq.(7) into Eq.(6) we obtain

$$\nabla_\theta \left[-\mathbb{E}_{p_\theta(x|y)p(y)} [\log q_{\phi_0}^r(y|x)] \right] \Big|_{\theta=\theta_0} = \nabla_\theta \left[\frac{1}{2} \text{KL}(p_{g_\theta} \| p_{data}) - \text{JSD}(p_{g_\theta} \| p_{data}) \right] \Big|_{\theta=\theta_0}, \quad (8)$$

which gives simplified explanations of the training dynamics and the missing mode issue only when the discriminator meets certain optimality criteria. Our generalized result enables understanding of broader situations. For instance, when the discriminator distribution $q_{\phi_0}(y|x)$ gives uniform guesses, or when $p_{g_\theta} = p_{data}$ that is indistinguishable by the discriminator, the gradients of the KL and JSD terms in Eq.(6) cancel out, which stops the generator learning.

InfoGAN Chen et al. [8] developed InfoGAN for disentangled representation learning which additionally recovers (part of) the latent code z given example x . This can be straightforwardly formulated in our framework by introducing an extra conditional $q_\eta(z|x, y)$ parameterized by η . As discussed above, GANs assume a degenerated code space for real examples, thus $q_\eta(z|x, y=1)$ is fixed without free parameters to learn, and η is only associated to $y=0$. The InfoGAN is then recovered by combining $q_\eta(z|x, y)$ with $q(y|x)$ in Eq.(3) to perform full reconstruction of both z and y :

$$\begin{aligned} \max_\phi \mathcal{L}_\phi &= \mathbb{E}_{p_\theta(x|y)p(y)} [\log q_\eta(z|x, y) q_\phi(y|x)] \\ \max_{\theta, \eta} \mathcal{L}_{\theta, \eta} &= \mathbb{E}_{p_\theta(x|y)p(y)} [\log q_\eta(z|x, y) q_\phi^r(y|x)], \end{aligned} \quad (9)$$

where the ground-truth z to reconstruct is sampled from the prior $p(z|y)$ and encapsulated in the implicit distribution $p_\theta(x|y)$. The model is expressed as graphical model in Figure 3(a). Let $q^r(x|z, y) \propto q_{\eta_0}(z|x, y) q_{\phi_0}^r(y|x) p_{\theta_0}(x)$, the result in the form of Eq.(6) still holds by replacing $q_{\phi_0}^r(y|x)$ with $q_{\eta_0}(z|x, y) q_{\phi_0}^r(y|x)$, and $q^r(x|y)$ with $q^r(x|z, y)$:

$$\begin{aligned} \nabla_\theta \left[-\mathbb{E}_{p_\theta(x|y)p(y)} [\log q_{\eta_0}(z|x, y) q_{\phi_0}^r(y|x)] \right] \Big|_{\theta=\theta_0} = \\ \nabla_\theta \left[\mathbb{E}_{p(y)} [\text{KL}(p_\theta(x|y) \| q^r(x|z, y))] - \text{JSD}(p_\theta(x|y=0) \| p_\theta(x|y=1)) \right] \Big|_{\theta=\theta_0}, \end{aligned} \quad (10)$$

AAE/PM/CycleGAN As a side result, the idea of interpreting data space x as latent immediately discovers relations between InfoGAN with Adversarial Autoencoder (AAE) [35] and Predictability Minimization (PM) [51]. That is, InfoGAN is precisely an AAE that treats the data space x as latent and to be adversarially regularized while the code space z as visible. Figure 3(c) shows the graphical model of AAE obtained by simply swapping x and z in InfoGAN. We defer the detailed formulations of AAE to the supplementary materials. Further, instead of considering x and z as data and code spaces respectively, if we let x and z be data spaces of two modalities, and combine the objectives of InfoGAN and AAE as a joint model, we recover the cycleGAN model [57] which performs transformation between the two modalities. More details are provided in the supplements.

3.3 Variational Autoencoders (VAEs)

We next explore the second family of deep generative model learning algorithms. The resemblance of GAN generator learning to variational inference as shown in Eq.(6) suggests strong relations between VAEs [28] and GANs. We build correspondence between the two approaches, and show that VAEs are basically minimizing a KL divergence in an opposite direction, with a degenerated adversarial discriminator.

The conventional definition of VAEs is written as:

$$\max_{\theta, \eta} \mathcal{L}_{\theta, \eta}^{\text{vae}} = \mathbb{E}_{p_{\text{data}}(\mathbf{x})} [\mathbb{E}_{\tilde{q}_{\eta}(\mathbf{z}|\mathbf{x})} [\log \tilde{p}_{\theta}(\mathbf{x}|\mathbf{z})] - \text{KL}(\tilde{q}_{\eta}(\mathbf{z}|\mathbf{x}) \parallel \tilde{p}(\mathbf{z}))], \quad (11)$$

where $\tilde{p}_{\theta}(\mathbf{x}|\mathbf{z})$ is the generator, $\tilde{q}_{\eta}(\mathbf{z}|\mathbf{x})$ the inference model, and $\tilde{p}(\mathbf{z})$ the prior over \mathbf{z} . The parameters to learn are intentionally denoted with the notations of corresponding modules in GANs. At first glance, VAEs appear to differ from GANs greatly as they use only real examples and lack adversarial mechanism. However, our interpretation shows VAEs indeed include a degenerated adversarial discriminator that blocks out generated samples from contributing to training.

Specifically, we again introduce the real/fake variable y . Further assume a perfect discriminator $q_*(y|\mathbf{x})$ which always predicts $y = 1$ with probability 1 given real examples, and $y = 0$ given generated samples. Again, for notational simplicity, let $q_*^r(y|\mathbf{x}) = q_*(1 - y|\mathbf{x})$ be the reversed distribution.

Lemma 2. *Let $p_{\theta}(\mathbf{z}, y|\mathbf{x}) \propto p_{\theta}(\mathbf{x}|\mathbf{z}, y)p(\mathbf{z}|y)p(y)$. Therefore, (omitting the constant scale factor 2)*

$$\begin{aligned} \mathcal{L}_{\theta, \eta}^{\text{vae}} &= \mathbb{E}_{p_{\theta_0}(\mathbf{x})} \left[\mathbb{E}_{q_{\eta}(\mathbf{z}|\mathbf{x}, y)q_*^r(y|\mathbf{x})} [\log p_{\theta}(\mathbf{x}|\mathbf{z}, y)] - \text{KL}(q_{\eta}(\mathbf{z}|\mathbf{x}, y)q_*^r(y|\mathbf{x}) \parallel p(\mathbf{z}|y)p(y)) \right] \\ &= \mathbb{E}_{p_{\theta_0}(\mathbf{x})} \left[-\text{KL}(q_{\eta}(\mathbf{z}|\mathbf{x}, y)q_*^r(y|\mathbf{x}) \parallel p_{\theta}(\mathbf{z}, y|\mathbf{x})) \right]. \end{aligned} \quad (12)$$

Here most of the components have exact correspondences (and the same definitions) in GANs and InfoGAN, except that the generation distribution $p_{\theta}(\mathbf{x}|\mathbf{z}, y)$ differs slightly from its counterpart $p_{\theta}(\mathbf{x}|y)$ in Eq.(4) to additionally account for the uncertainty of generating \mathbf{x} given \mathbf{z} :

$$p_{\theta}(\mathbf{x}|\mathbf{z}, y) = \begin{cases} \tilde{p}_{\theta}(\mathbf{x}|\mathbf{z}) & y = 0 \\ p_{\text{data}}(\mathbf{x}) & y = 1. \end{cases} \quad (13)$$

The resulting KL divergence closely relates to that in GANs (Eq.6) and InfoGAN (Eq.10), with the generator parameters θ and the inference parameters η (and ϕ) placed in the opposite directions, and with inverted hidden/visible treatments of (\mathbf{z}, y) and \mathbf{x} . Figure 3(b) shows the graphical model of the new interpretation of VAEs, where the only difference from InfoGAN (Figure 3(a)) is swapping the solid-line arrows (generative process) and dashed-line arrows (inference). In section 6, we give a general discussion that the difference between GANs and VAEs in latent/visible treatments is relatively minor.

The proof of Lemma 2 is provided in the supplementary materials. Intuitively, recall that for the real example domain with $y = 1$, both $q_{\eta}(\mathbf{z}|\mathbf{x}, y = 1)$ and $p_{\theta}(\mathbf{x}|\mathbf{z}, y = 1)$ are constant distributions. Therefore, with fake sample \mathbf{x} generated from $p_{\theta_0}(\mathbf{x})$, the reversed perfect discriminator $q_*^r(y|\mathbf{x})$ always gives prediction $y = 1$, making the reconstruction loss on fake samples degenerated to a constant. Hence only real examples, where q_*^r predicts $y = 0$ with probability 1, are effective for learning, which is identical to Eq.(11). We extend VAEs to also leverage fake samples in section 4.

VAE/GAN Joint Models Previous works have explored combination of VAEs and GANs. This can be naturally motivated by the asymmetric behaviors of the KL divergences that the two algorithms aim to optimize respectively. Specifically, the VAE/GAN model [32] that improves the sharpness of VAE generated images can be alternatively motivated by remedying the mode covering behavior of the KL in VAEs. That is, the KL tends to drive the generative model to cover all modes of the data distribution as well as regions with small values of p_{data} , resulting in blurred, implausible samples. Incorporation of GAN objectives alleviates the issue as the inverted KL enforces the generator to focus on meaningful data modes. From the other perspective, augmenting GANs with VAE objectives helps addressing the mode missing problem, which justifies the intuition of [6].

Components	ADA	GANs	VAEs
\mathbf{x}	features	data/generations	data/generations
y	domain indicator	real/fake indicator	(degenerated) real/fake indicator
\mathbf{z}	data examples	code vector	code vector
$p_\theta(\mathbf{x} y)$	feature distr.	generation distr., Eq.4	$p_\theta(\mathbf{x} \mathbf{z}, y)$, generation distr., Eq.13
$q_\phi(y \mathbf{x})$	discriminator	discriminator	$q_*(y \mathbf{x})$, degenerated discriminator
$q_\eta(\mathbf{z} \mathbf{x}, y)$	—	infer net (InfoGAN)	infer net
$p_{\theta_0}(\mathbf{x})$ (lemma 1)	same of GANs	prior of \mathbf{x}	prior of \mathbf{x}
KLD to minimize	same as GANs	$\text{KL}(p_\theta(\mathbf{x} y) \ q^r(\mathbf{x} y))$	$\text{KL}(q_\eta(\mathbf{z} \mathbf{x}, y) q_*^r(y \mathbf{x}) \ p_\theta(\mathbf{z}, y \mathbf{x}))$

Table 1: Correspondence between different approaches in the proposed formulation.

3.4 Wake Sleep Algorithm (WS)

We next discuss the connections of GANs and VAEs to the classic wake-sleep algorithm [21] which was proposed for learning deep generative models such as Helmholtz machines [11]. WS consists of wake phase and sleep phase, which optimize the generative model and inference model, respectively. We follow the above notations, and introduce new notations \mathbf{h} to denote general latent variables and λ for general parameters. The wake sleep algorithm is thus written as:

$$\begin{aligned}
\text{Wake : } & \max_{\theta} \mathbb{E}_{q_{\lambda}(\mathbf{h}|\mathbf{x})p_{data}(\mathbf{x})} [\log p_{\theta}(\mathbf{x}|\mathbf{h})] \\
\text{Sleep : } & \max_{\lambda} \mathbb{E}_{p_{\theta}(\mathbf{x}|\mathbf{h})p(\mathbf{h})} [\log q_{\lambda}(\mathbf{h}|\mathbf{x})] .
\end{aligned} \tag{14}$$

The wake phase updates the generator parameters θ by fitting $p_{\theta}(\mathbf{x}|\mathbf{h})$ to the real data and hidden code inferred by the inference model $q_{\lambda}(\mathbf{h}|\mathbf{x})$. On the other hand, the sleep phase updates the parameters λ based on the generated samples from the generator.

The relations between WS and VAEs are clear in previous discussions [4, 28]. Indeed, WS was originally proposed to minimize the variational lower bound as in VAEs (Eq.11) with sleep phase approximation [21]. Alternatively, VAEs can be seen as extending the wake phase. Specifically, if we let \mathbf{h} be \mathbf{z} and λ be η , the wake phase objective recovers VAEs (Eq.11) in terms of generator optimization (i.e., optimizing θ). Therefore, we can see VAEs as generalizing the wake phase by also optimizing the inference model q_{η} , with additional prior regularization on code \mathbf{z} .

On the other hand, our interpretation of GANs reveals close resemblance to the sleep phase. To make this clearer, let \mathbf{h} be y and λ be ϕ . This results in a sleep phase objective identical to that of optimizing the discriminator q_{ϕ} in Eq.(3), which is to reconstruct y given sample \mathbf{x} . We thus can view GANs as generalizing the sleep phase by also optimizing the generative model p_{θ} to reconstruct reversed y . InfoGAN (Eq.9) further extends the correspondence to reconstruction of latents \mathbf{z} .

3.5 Summary

We have established close relations between ADA, GANs, VAEs, WS, and many model variants through the proposed formulations. Table 1 summarizes the correspondence of each components in the approaches. In particular, the symmetry of GANs and VAEs in terms of minimizing KL divergences in opposite directions strongly relates to the symmetry of the sleep and wake phases in the wake-sleep algorithm. Besides, the opposite KL divergences formally explain common observations when training GANs and VAEs, such as the mode missing and mode covering behaviors that have led to different practical issues and motivated various model extensions. Also, our analysis of GANs does not rely on the commonly assumed optimality of the discriminators (Lemma 1), which can give new insights of model training in practice.

4 Applications

Our new interpretation not only reveals a unified statistical insight and the connections underlying the existing approaches, but also facilitates to draw inspirations across the two classes of algorithms to develop enhanced variants. In this section, we give example extensions to GANs and VAEs, respectively, by directly importing ideas from the other approaches.

4.1 Importance Weighted GANs (IWGAN)

Burda et al. [5] proposed importance weighted autoencoders (IWAE) that maximizes a tighter lower bound on the marginal likelihood. In our framework it is straightforward to develop importance weighted GANs by copying the derivations of IWAE side by side with little adaptations. Here we outline the development and give the details in the supplementary materials.

The variational inference interpretation of the objective in Eq.(6) suggests GANs can be approximately viewed as maximizing a lower bound of the marginal likelihood on y (putting aside the negative JSD term):

$$\begin{aligned}\log q(y) &= \log \int p_\theta(\mathbf{x}|y) \frac{q_{\phi_0}^r(y|\mathbf{x})p_{\theta_0}(\mathbf{x})}{p_\theta(\mathbf{x}|y)} d\mathbf{x} \\ &\geq \int p_\theta(\mathbf{x}|y) \log \frac{q_{\phi_0}^r(y|\mathbf{x})p_{\theta_0}(\mathbf{x})}{p_\theta(\mathbf{x}|y)} d\mathbf{x} = -\text{KL}(p_\theta(\mathbf{x}|y) \| q^r(\mathbf{x}|y)) + \text{const.}\end{aligned}\quad (15)$$

Following [5], we derive a tighter lower bound through a k -sample importance weighting estimate of the log-likelihood:

$$\log q(y) \geq \mathbb{E} \left[\log \frac{1}{k} \sum_{i=1}^k \frac{q_{\phi_0}^r(y|\mathbf{x}_i)p_{\theta_0}(\mathbf{x}_i)}{p_\theta(\mathbf{x}_i|y)} \right] = \mathbb{E} \left[\log \frac{1}{k} \sum_{i=1}^k w_i \right] := \mathcal{L}_k(y) \quad (16)$$

where $w_i = \frac{q_{\phi_0}^r(y|\mathbf{x}_i)p_{\theta_0}(\mathbf{x}_i)}{p_\theta(\mathbf{x}_i|y)}$ is the unnormalized importance weight. The lower bound of Eq.(15) is recovered with $k = 1$. Taking derivative of $\mathcal{L}_k(y)$ and applying the reparameterization trick on samples \mathbf{x}_i , we have:

$$\nabla_\theta \mathcal{L}_k(y) = \mathbb{E}_{\mathbf{z}_1, \dots, \mathbf{z}_k \sim p(\mathbf{z}|y)} \left[\sum_{i=1}^k \widetilde{w}_i \nabla_\theta \log w(y, \mathbf{x}(\mathbf{z}_i, \boldsymbol{\theta}), \boldsymbol{\theta}) \right]. \quad (17)$$

Here $\widetilde{w}_i = w_i / \sum_{i=1}^k w_i$, in which w_i can be approximated by assuming optimal discriminator distribution:

$$w_i \approx \frac{q_{\phi_0}^r(y|\mathbf{x}_i)}{q_{\phi_0}(y|\mathbf{x}_i)}. \quad (18)$$

The derivative of w_i at $\boldsymbol{\theta}_0$ is computed as:

$$\nabla_\theta \log w(y, \mathbf{x}(\mathbf{z}_i, \boldsymbol{\theta}), \boldsymbol{\theta})|_{\boldsymbol{\theta}=\boldsymbol{\theta}_0} = \nabla_\theta \left(\log q_{\phi_0}^r(y|\mathbf{x}(\mathbf{z}_i, \boldsymbol{\theta})) + \log \frac{p_{\theta_0}(\mathbf{x}_i)}{p_\theta(\mathbf{x}_i|y)} \right)|_{\boldsymbol{\theta}=\boldsymbol{\theta}_0}. \quad (19)$$

In analog to the standard GANs which omit priors by subtracting the JSD term (Eq.6), we also omit the second term in the derivative relevant to the prior $p_{\theta_0}(\mathbf{x})$. The resulting update rule for the generator is thus of the following form:

$$\nabla_\theta \mathcal{L}_k(y) = \mathbb{E}_{\mathbf{z}_1, \dots, \mathbf{z}_k \sim p(\mathbf{z}|y)} \left[\sum_{i=1}^k \widetilde{w}_i \nabla_\theta \log q_{\phi_0}^r(y|\mathbf{x}(\mathbf{z}_i, \boldsymbol{\theta})) \right]. \quad (20)$$

As in GANs, only $y = 0$ (i.e., generated samples) is effective for learning the parameters $\boldsymbol{\theta}$. Intuitively, the algorithm assigns higher weights to those samples that are more realistic and fool the discriminator better, which is consistent to IWAE that emphasizes more on code states providing better reconstructions. Hjelm et al. [22], Che et al. [7] developed a similar sample weighting scheme for maximum likelihood training of the generator. In practice, the k samples in Eq.(20) correspond to a minibatch of samples in standard GAN update. Thus the only computational cost added by the importance weighting method is evaluating the weight for each sample, which is generally negligible. The discriminator is trained in the same way as in the standard GANs.

4.2 Adversary Activated VAEs (AAVAE)

In our formulation, VAEs include a degenerated adversarial discriminator which blocks out generated samples from contributing to model learning. We enable adaptive incorporation of fake samples by activating the adversarial mechanism. Again, derivations are straightforward by making symbolic analog to GANs.

We replace the perfect discriminator $q_*(y|\mathbf{x})$ in vanilla VAEs with the discriminator network $q_\phi(y|\mathbf{x})$ parameterized with ϕ as in GANs, resulting in an adapted objective of Eq.(12):

$$\max_{\theta, \eta} \mathcal{L}_{\theta, \eta}^{\text{aavae}} = \mathbb{E}_{p_{\theta_0}(\mathbf{x})} \left[\mathbb{E}_{q_\eta(\mathbf{z}|\mathbf{x}, y) q_\phi^r(y|\mathbf{x})} [\log p_\theta(\mathbf{x}|\mathbf{z}, y)] - \text{KL}(q_\eta(\mathbf{z}|\mathbf{x}, y) q_\phi^r(y|\mathbf{x}) \| p(\mathbf{z}|y)p(y)) \right]. \quad (21)$$

The form of Eq.(21) is precisely symmetric to the objective of InfoGAN in Eq.(9) with the additional KL prior regularization. Before analyzing the effect of adding the learnable discriminator, we first look at how the discriminator is learned. In analog to GANs as in Eqs.(3) and (9), the objective of optimizing ϕ is obtained by simply replacing the inverted distribution $q_\phi^r(y|\mathbf{x})$ with $q_\phi(y|\mathbf{x})$:

$$\max_{\phi} \mathcal{L}_{\phi}^{\text{aavae}} = \mathbb{E}_{p_{\theta_0}(\mathbf{x})} \left[\mathbb{E}_{q_\eta(\mathbf{z}|\mathbf{x}, y) q_\phi(y|\mathbf{x})} [\log p_\theta(\mathbf{x}|\mathbf{z}, y)] - \text{KL}(q_\eta(\mathbf{z}|\mathbf{x}, y) q_\phi(y|\mathbf{x}) \| p(\mathbf{z}|y)p(y)) \right]. \quad (22)$$

Intuitively, the discriminator is trained to distinguish between real and fake instances by predicting appropriate y that selects the components of $q_\eta(\mathbf{z}|\mathbf{x}, y)$ and $p_\theta(\mathbf{x}|\mathbf{z}, y)$ to best reconstruct \mathbf{x} . The difficulty of Eq.(22) is that $p_\theta(\mathbf{x}|\mathbf{z}, y=1) = p_{\text{data}}(\mathbf{x})$ is an implicit distribution which is intractable for likelihood evaluation. We thus use the alternative objective as in GANs to train a binary classifier:

$$\max_{\phi} \mathcal{L}_{\phi}^{\text{aavae}} = \mathbb{E}_{p_\theta(\mathbf{x}|\mathbf{z}, y)p(\mathbf{z}|y)p(y)} [\log q_\phi(y|\mathbf{x})]. \quad (23)$$

The activated discriminator enables an effective data selection mechanism. First, AAVAE uses not only real examples, but also generated samples for training. Each sample is weighted by the inverted discriminator $q_\phi^r(y|\mathbf{x})$, so that only those samples that resemble real data and successfully fool the discriminator will be incorporated for training. This is consistent with the importance weighting strategy in IWGAN. Second, real examples are also weighted by $q_\phi^r(y|\mathbf{x})$. An example receiving large weight indicates it is easily recognized by the discriminator, which further indicates the example is hard to be simulated from the generator. That is, AAVAE emphasizes more on harder examples.

5 Experiments

We perform extensive quantitative experiments to evaluate the importance weighting method for GANs and the adversary activating method for VAEs. To show the generality of the imported ideas, we apply the extensions to vanilla models as well as several popular variants, and obtain greatly improved results.

5.1 Importance Weighted GANs

We extend both vanilla GANs and class-conditional GANs (CGAN) with the importance weighting method. The base GAN model is implemented with the DCGAN architecture and hyperparameter setting [48]. We do not tune the hyperparameters for the importance weighted extensions. We use MNIST and SVHN for evaluation. For vanilla GANs and its IW extension, we measure inception scores [50] on the generated samples. We train deep residual networks [19] provided in the tensorflow library as evaluation networks, which achieve inception scores of 9.09 and 6.55 on the test sets of MNIST and SVHN, respectively. For conditional GANs we evaluate the accuracy of conditional generation [25]. That is, we generate samples given class labels, and then use the pre-trained classifier to predict class labels of the generated samples. The accuracy is calculated as the percentage of the predictions that match the conditional labels. The evaluation networks achieve accuracy of 0.990 and 0.902 on the test sets of MNIST and SVHN, respectively.

Table 2, left panel, shows the inception scores of GANs and IW-GAN, and the middle panel gives the classification accuracy of the conditional GANs and its importance weighted extension IW-CGAN. We report the averaged results \pm one standard deviation over 5 runs. We see that the importance weighting strategy gives consistent improvements over the base models.

5.2 Adversary Activated VAEs

We apply the adversary activating method on vanilla VAEs, class-conditional VAEs (CVAE), and semi-supervised VAEs (SVAE) [29]. We evaluate on the MNIST data. The generator networks have the same architecture as the generators in GANs in the above experiments, with sigmoid activation

	MNIST	SVHN		MNIST	SVHN		1%	10%
GAN	8.34 \pm .03	5.18 \pm .03	CGAN	0.985 \pm .002	0.797 \pm .005	SVAE	0.9412	0.9768
IWGAN	8.45\pm.04	5.34\pm.03	IWCGAN	0.987\pm.002	0.798\pm.006	AASVAE	0.9425	0.9797

Table 2: **Left:** Inception scores of vanilla GANs and the importance weighted extension. **Middle:** Classification accuracy of the generations by class-conditional GANs and the IW extension. **Right:** Classification accuracy of semi-supervised VAEs and the adversary activated extension on the MNIST test set, with varying size of real labeled training examples.

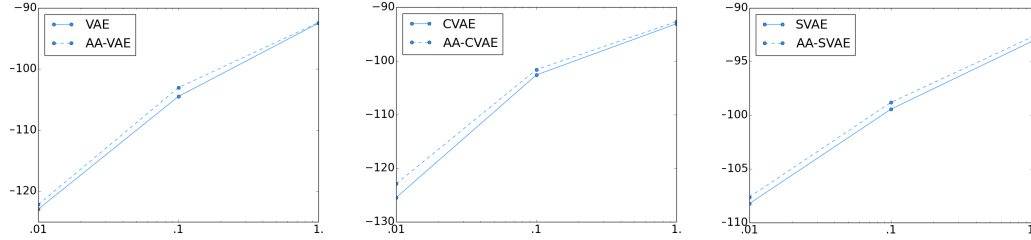


Figure 4: Lower bound values on the MNIST test set. X-axis represents the ratio of training data used for learning (0.01, 0.1, and 1.). Y-axis represents the value of lower bound. Solid lines represent the base models; dashed lines represent the adversary activated models. **Left:** VAE vs. AA-VAE. **Middle:** CVAE vs. AA-CVAE. **Right:** SVAE vs. AA-SVAE, where remaining training data are used as unsupervised data.

functions on the last layer to compute the means of Bernoulli distributions over pixels. The inference networks, discriminators, and the classifier in SVAE share the same architecture as the discriminators in the GAN experiments.

We evaluate the lower bound value on the test set, with varying number of real training examples. For each minibatch of real examples we generate equal number of fake samples for training. In the experiments we found it is generally helpful to smooth the discriminator distributions by setting the temperature of the output sigmoid function larger than 1. This basically encourages the use of fake data for learning. We select the best temperature from $\{1, 1.5, 3, 5\}$ through cross-validation. We do not tune other hyperparameters for the adversary activated extensions. Figure 4 shows the results of activating the adversary mechanism on the VAE models. We see that the adversary activated models consistently outperform their respective base models. Generally, larger improvement can be obtained with smaller set of real training data. Table 2, right panel, further shows the classification accuracy of semi-supervised VAE and its adversary activated variants with different size of labeled training data. We can observe improved performance of the AA-SVAE model. The full results of standard deviations are reported in the supplementary materials.

6 Discussions

Our new interpretations of GANs and VAEs have revealed strong connections between them, and linked the emerging new approaches to the classic wake-sleep algorithm. The generality of the proposed formulation offers a unified statistical insight of the broad landscape of deep generative modeling, and encourages mutual exchange of improvement ideas across research lines. It is interesting to further generalize the framework to connect to other learning paradigms such as reinforcement learning as previous works have started exploration [14, 45]. GANs simultaneously learn a metric (defined by the discriminator) to guide the generator learning, which resembles the iterative teacher-student distillation framework [23, 24] where a teacher network is simultaneously learned from structured knowledge (e.g., logic rules) and provides knowledge-informed learning signals for student networks of interest. It will be intriguing to build formal connections between these approaches and enable incorporation of structured knowledge in deep generative modeling.

Symmetric view of generation and inference Traditional modeling approaches usually distinguish between latent and visible variables clearly and treat them in very different ways. One of the

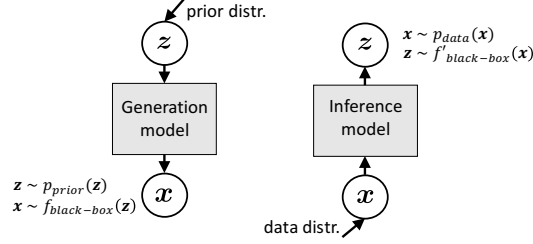


Figure 5: Symmetric view of generation and inference. There is little difference of the two processes in terms of formulation: with implicit distribution modeling, both processes only need to perform simulation through black-box neural transformations between the latent and visible spaces.

key thoughts in our formulation is that it is not necessary to make clear boundary between the two types of variables (and between generation and inference), but instead, treating them as a symmetric pair helps with modeling and understanding. For instance, we treat the generation space x in GANs as latent, which immediately reveals the connection between GANs and adversarial domain adaptation, and provides a variational inference interpretation of the generation. A second example is the classic wake-sleep algorithm, where the wake phase reconstructs visibles conditioned on latents, while the sleep phase reconstructs latents conditioned on visibles (i.e., generated samples). Hence, visible and latent variables are treated in a completely symmetric manner.

Furthermore, the newly emerging tools such as implicit distribution modeling and black-box neural transformations have enabled undifferentiated formulation of generation and inference (Figure 5). Generally, we have prior distributions over latent space, and empirical data distributions over visible space. Both are pre-defined and can be easily sampled from. There are two major differences.

- Empirical data distributions are usually implicit, i.e., easy to sample from but intractable for evaluating likelihood. In contrast, priors are usually defined as explicit distributions, amiable for likelihood evaluation.
- The complexity of the two distributions are different. Visible space is usually complex while latent space tends (or is designed) to be simpler.

However, the adversarial approach in GANs and other techniques such as density ratio estimation [39] and approximate Bayesian computation [3] have provided useful tools to bridge the gap in the first point. For instance, implicit generative models such as GANs require only simulation of the generative process without explicit likelihood evaluation, hence the prior distributions over latent variables are used in the same way as the empirical data distributions, namely, generating samples from the distributions. For explicit likelihood-based models, adversarial autoencoder (AAE) leverages the adversarial approach to allow implicit prior distributions over latent space. Besides, a few most recent work [36, 54, 26, 49] extends VAEs by using implicit variational distributions as the inference model. Indeed, the reparameterization trick in VAEs already resembles construction of implicit variational distributions (as also seen in the derivations of IWGANs in Eq.17). In these algorithms, adversarial approach is used to replace intractable minimization of the KL divergence between implicit variational distributions and priors.

The second difference in terms of space complexity guides us to choose appropriate tools (e.g., adversarial approach v.s. reconstruction optimization, etc) to minimize the distance between distributions to learn and their targets. However, the tools chosen do not affect the underlying modeling mechanism. For instance, VAEs and adversarial autoencoder both regularize the model by minimizing the distance between the variational posterior and certain prior, though VAEs choose KL divergence loss while AAE selects adversarial loss.

We can further extend the symmetric treatment of visible/latent x/z pair to data/label x/t pair, leading to a unified view of the generative and discriminative paradigms for unsupervised and semi-supervised learning. Specifically, conditional generative models create (data, label) pairs by generating data x given label t . These pairs can be used for classifier training [25, 42]. In parallel, discriminative approaches such as knowledge distillation [23, 20] create (data, label) pairs by generating label t conditioned on data x . With the symmetric view of x and t spaces, and neural network based black-box mappings across spaces, we can see the two approaches are essentially the same.

References

- [1] M. Arjovsky and L. Bottou. Towards principled methods for training generative adversarial networks. In *ICLR*, 2017.
- [2] S. Arora, R. Ge, Y. Liang, T. Ma, and Y. Zhang. Generalization and equilibrium in generative adversarial nets (GANs). *arXiv preprint arXiv:1703.00573*, 2017.
- [3] M. A. Beaumont, W. Zhang, and D. J. Balding. Approximate Bayesian computation in population genetics. *Genetics*, 162(4):2025–2035, 2002.
- [4] J. Bornschein and Y. Bengio. Reweighted wake-sleep. *arXiv preprint arXiv:1406.2751*, 2014.
- [5] Y. Burda, R. Grosse, and R. Salakhutdinov. Importance weighted autoencoders. *arXiv preprint arXiv:1509.00519*, 2015.
- [6] T. Che, Y. Li, A. P. Jacob, Y. Bengio, and W. Li. Mode regularized generative adversarial networks. *ICLR*, 2017.
- [7] T. Che, Y. Li, R. Zhang, R. D. Hjelm, W. Li, Y. Song, and Y. Bengio. Maximum-likelihood augmented discrete generative adversarial networks. *arXiv preprint arXiv:1702.07983*, 2017.
- [8] X. Chen, Y. Duan, R. Houthoofd, J. Schulman, I. Sutskever, and P. Abbeel. InfoGAN: Interpretable representation learning by information maximizing generative adversarial nets. In *NIPS*, pages 2172–2180, 2016.
- [9] X. Chen, Y. Sun, B. Athiwaratkun, C. Cardie, and K. Weinberger. Adversarial deep averaging networks for cross-lingual sentiment classification. *arXiv preprint arXiv:1606.01614*, 2016.
- [10] X. Chen, D. P. Kingma, T. Salimans, Y. Duan, P. Dhariwal, J. Schulman, I. Sutskever, and P. Abbeel. Variational lossy autoencoder. *ICLR*, 2017.
- [11] P. Dayan, G. E. Hinton, R. M. Neal, and R. S. Zemel. The helmholtz machine. *Neural computation*, 7(5):889–904, 1995.
- [12] A. P. Dempster, N. M. Laird, and D. B. Rubin. Maximum likelihood from incomplete data via the EM algorithm. *Journal of the royal statistical society. Series B (methodological)*, pages 1–38, 1977.
- [13] G. K. Dziugaite, D. M. Roy, and Z. Ghahramani. Training generative neural networks via maximum mean discrepancy optimization. *arXiv preprint arXiv:1505.03906*, 2015.
- [14] C. Finn, P. Christiano, P. Abbeel, and S. Levine. A connection between generative adversarial networks, inverse reinforcement learning, and energy-based models. *arXiv preprint arXiv:1611.03852*, 2016.
- [15] Y. Ganin, E. Ustinova, H. Ajakan, P. Germain, H. Larochelle, F. Laviolette, M. Marchand, and V. Lempitsky. Domain-adversarial training of neural networks. *Journal of Machine Learning Research*, 17(59):1–35, 2016.
- [16] I. Goodfellow, J. Pouget-Abadie, M. Mirza, B. Xu, D. Warde-Farley, S. Ozair, A. Courville, and Y. Bengio. Generative adversarial nets. In *NIPS*, pages 2672–2680, 2014.
- [17] P. Goyal, Z. Hu, X. Liang, C. Wang, and E. Xing. Nonparametric variational auto-encoders for hierarchical representation learning. In *ICCV*, 2017.
- [18] M. U. Gutmann, R. Dutta, S. Kaski, and J. Corander. Statistical inference of intractable generative models via classification. *arXiv preprint arXiv:1407.4981*, 2014.
- [19] K. He, X. Zhang, S. Ren, and J. Sun. Deep residual learning for image recognition. In *Proceedings of the IEEE Conference on Computer Vision and Pattern Recognition*, pages 770–778, 2016.
- [20] G. Hinton, O. Vinyals, and J. Dean. Distilling the knowledge in a neural network. *arXiv preprint arXiv:1503.02531*, 2015.

- [21] G. E. Hinton, P. Dayan, B. J. Frey, and R. M. Neal. The "wake-sleep" algorithm for unsupervised neural networks. *Science*, 268(5214):1158, 1995.
- [22] R. D. Hjelm, A. P. Jacob, T. Che, K. Cho, and Y. Bengio. Boundary-seeking generative adversarial networks. *arXiv preprint arXiv:1702.08431*, 2017.
- [23] Z. Hu, X. Ma, Z. Liu, E. Hovy, and E. Xing. Harnessing deep neural networks with logic rules. In *ACL*, 2016.
- [24] Z. Hu, Z. Yang, R. Salakhutdinov, and E. P. Xing. Deep neural networks with massive learned knowledge. In *EMNLP*, 2016.
- [25] Z. Hu, Z. Yang, X. Liang, R. Salakhutdinov, and E. P. Xing. Toward controlled generation of text. In *ICML*, 2017.
- [26] F. Huszár. Variational inference using implicit distributions. *arXiv preprint arXiv:1702.08235*, 2017.
- [27] M. I. Jordan, Z. Ghahramani, T. S. Jaakkola, and L. K. Saul. An introduction to variational methods for graphical models. *Machine learning*, 37(2):183–233, 1999.
- [28] D. P. Kingma and M. Welling. Auto-encoding variational Bayes. *arXiv preprint arXiv:1312.6114*, 2013.
- [29] D. P. Kingma, S. Mohamed, D. J. Rezende, and M. Welling. Semi-supervised learning with deep generative models. In *NIPS*, pages 3581–3589, 2014.
- [30] T. D. Kulkarni, W. F. Whitney, P. Kohli, and J. Tenenbaum. Deep convolutional inverse graphics network. In *NIPS*, pages 2539–2547, 2015.
- [31] H. Larochelle and I. Murray. The neural autoregressive distribution estimator. In *Proceedings of the Fourteenth International Conference on Artificial Intelligence and Statistics*, pages 29–37, 2011.
- [32] A. B. L. Larsen, S. K. Sønderby, H. Larochelle, and O. Winther. Autoencoding beyond pixels using a learned similarity metric. *arXiv preprint arXiv:1512.09300*, 2015.
- [33] Y. Li, K. Swersky, and R. Zemel. Generative moment matching networks. In *Proceedings of the 32nd International Conference on Machine Learning*, pages 1718–1727, 2015.
- [34] X. Liang, Z. Hu, H. Zhang, C. Gan, and E. P. Xing. Recurrent topic-transition GAN for visual paragraph generation. In *ICCV*, 2017.
- [35] A. Makhzani, J. Shlens, N. Jaitly, I. Goodfellow, and B. Frey. Adversarial autoencoders. *arXiv preprint arXiv:1511.05644*, 2015.
- [36] L. Mescheder, S. Nowozin, and A. Geiger. Adversarial variational Bayes: Unifying variational autoencoders and generative adversarial networks. *arXiv preprint arXiv:1701.04722*, 2017.
- [37] L. Metz, B. Poole, D. Pfau, and J. Sohl-Dickstein. Unrolled generative adversarial networks. *ICLR*, 2017.
- [38] A. Mnih and K. Gregor. Neural variational inference and learning in belief networks. *arXiv preprint arXiv:1402.0030*, 2014.
- [39] S. Mohamed and B. Lakshminarayanan. Learning in implicit generative models. *arXiv preprint arXiv:1610.03483*, 2016.
- [40] R. M. Neal. Connectionist learning of belief networks. *Artificial intelligence*, 56(1):71–113, 1992.
- [41] S. Nowozin, B. Cseke, and R. Tomioka. f-GAN: Training generative neural samplers using variational divergence minimization. In *Advances in Neural Information Processing Systems*, pages 271–279, 2016.

- [42] A. Odena, C. Olah, and J. Shlens. Conditional image synthesis with auxiliary classifier GANs. *ICML*, 2017.
- [43] A. v. d. Oord, N. Kalchbrenner, and K. Kavukcuoglu. Pixel recurrent neural networks. *arXiv preprint arXiv:1601.06759*, 2016.
- [44] J. Paisley, D. Blei, and M. Jordan. Variational Bayesian inference with stochastic search. In *ICML*, 2012.
- [45] D. Pfau and O. Vinyals. Connecting generative adversarial networks and actor-critic methods. *arXiv preprint arXiv:1610.01945*, 2016.
- [46] S. Purushotham, W. Carvalho, T. Nilanon, and Y. Liu. Variational recurrent adversarial deep domain adaptation. In *ICLR*, 2017.
- [47] L. Qin, Z. Zhang, H. Zhao, Z. Hu, and E. P. Xing. Adversarial connective-exploiting networks for implicit discourse relation classification. *arXiv preprint arXiv:1704.00217*, 2017.
- [48] A. Radford, L. Metz, and S. Chintala. Unsupervised representation learning with deep convolutional generative adversarial networks. *arXiv preprint arXiv:1511.06434*, 2015.
- [49] M. Rosca, B. Lakshminarayanan, D. Warde-Farley, and S. Mohamed. Variational approaches for auto-encoding generative adversarial networks. *arXiv preprint arXiv:1706.04987*, 2017.
- [50] T. Salimans, I. Goodfellow, W. Zaremba, V. Cheung, A. Radford, and X. Chen. Improved techniques for training GANs. In *NIPS*, pages 2226–2234, 2016.
- [51] J. Schmidhuber. Learning factorial codes by predictability minimization. *Neural Computation*, 4(6):863–879, 1992.
- [52] C. K. Sønderby, J. Caballero, L. Theis, W. Shi, and F. Huszár. Amortised MAP inference for image super-resolution. *ICLR*, 2017.
- [53] M. A. Tanner and W. H. Wong. The calculation of posterior distributions by data augmentation. *Journal of the American statistical Association*, 82(398):528–540, 1987.
- [54] D. Tran, R. Ranganath, and D. M. Blei. Deep and hierarchical implicit models. *arXiv preprint arXiv:1702.08896*, 2017.
- [55] A. van den Oord, N. Kalchbrenner, L. Espeholt, O. Vinyals, A. Graves, and K. Kavukcuoglu. Conditional image generation with pixelCNN decoders. In *Advances in Neural Information Processing Systems*, pages 4790–4798, 2016.
- [56] R. J. Williams. Simple statistical gradient-following algorithms for connectionist reinforcement learning. *Machine learning*, 8(3):229–256, 1992.
- [57] J.-Y. Zhu, T. Park, P. Isola, and A. A. Efros. Unpaired image-to-image translation using cycle-consistent adversarial networks. *arXiv preprint arXiv:1703.10593*, 2017.

A Adversarial Domain Adaptation (ADA)

ADA aims to transfer prediction knowledge learned from a source domain with labeled data to a target domain without labels, by learning domain-invariant features. Let $D_\phi(\mathbf{x}) = q_\phi(y|\mathbf{x})$ be the domain discriminator. The conventional formulation of ADA is as following:

$$\begin{aligned}\max_{\phi} \mathcal{L}_\phi &= \mathbb{E}_{\mathbf{x}=G_\theta(\mathbf{z}), \mathbf{z} \sim p(\mathbf{z}|y=1)} [\log D_\phi(\mathbf{x})] + \mathbb{E}_{\mathbf{x}=G_\theta(\mathbf{z}), \mathbf{z} \sim p(\mathbf{z}|y=0)} [\log(1 - D_\phi(\mathbf{x}))], \\ \max_{\theta} \mathcal{L}_\theta &= \mathbb{E}_{\mathbf{x}=G_\theta(\mathbf{z}), \mathbf{z} \sim p(\mathbf{z}|y=1)} [\log(1 - D_\phi(\mathbf{x}))] + \mathbb{E}_{\mathbf{x}=G_\theta(\mathbf{z}), \mathbf{z} \sim p(\mathbf{z}|y=0)} [\log D_\phi(\mathbf{x})].\end{aligned}\quad (24)$$

Further add the supervision objective of predicting label $t(\mathbf{z})$ of data \mathbf{z} in the source domain, with a classifier $f_\omega(t|\mathbf{x})$ parameterized with π :

$$\max_{\omega, \theta} \mathcal{L}_{\omega, \theta} = \mathbb{E}_{\mathbf{z} \sim p(\mathbf{z}|y=1)} [\log f_\omega(t(\mathbf{z})|G_\theta(\mathbf{z}))]. \quad (25)$$

We then obtain the conventional formulation of adversarial domain adaptation used or similar in [15, 46, 47, 9].

B Proof of Lemma 1

Proof.

$$\begin{aligned}\mathbb{E}_{p_\theta(\mathbf{x}|y)p(y)} [\log q^r(y|\mathbf{x})] &= \\ &- \mathbb{E}_{p(y)} [\text{KL}(p_\theta(\mathbf{x}|y) \| q^r(\mathbf{x}|y)) - \text{KL}(p_\theta(\mathbf{x}|y) \| p_{\theta_0}(\mathbf{x}))],\end{aligned}\quad (26)$$

where

$$\begin{aligned}\mathbb{E}_{p(y)} [\text{KL}(p_\theta(\mathbf{x}|y) \| p_{\theta_0}(\mathbf{x}))] &= \\ &= p(y=0) \cdot \text{KL}\left(p_\theta(\mathbf{x}|y=0) \left\| \frac{p_{\theta_0}(\mathbf{x}|y=0) + p_{\theta_0}(\mathbf{x}|y=1)}{2}\right.\right) \\ &+ p(y=1) \cdot \text{KL}\left(p_\theta(\mathbf{x}|y=1) \left\| \frac{p_{\theta_0}(\mathbf{x}|y=0) + p_{\theta_0}(\mathbf{x}|y=1)}{2}\right.\right).\end{aligned}\quad (27)$$

Note that $p_\theta(\mathbf{x}|y=0) = p_{g_\theta}(\mathbf{x})$, and $p_\theta(\mathbf{x}|y=1) = p_{data}(\mathbf{x})$. Let $p_{M_\theta} = \frac{p_{g_\theta} + p_{data}}{2}$. Eq.(27) can be simplified as:

$$\mathbb{E}_{p(y)} [\text{KL}(p_\theta(\mathbf{x}|y) \| p_{\theta_0}(\mathbf{x}))] = \frac{1}{2} \text{KL}(p_{g_\theta} \| p_{M_{\theta_0}}) + \frac{1}{2} \text{KL}(p_{data} \| p_{M_{\theta_0}}). \quad (28)$$

On the other hand,

$$\begin{aligned}\text{JSD}(p_{g_\theta} \| p_{data}) &= \frac{1}{2} \mathbb{E}_{p_{g_\theta}} \left[\log \frac{p_{g_\theta}}{p_{M_\theta}} \right] + \frac{1}{2} \mathbb{E}_{p_{data}} \left[\log \frac{p_{data}}{p_{M_\theta}} \right] \\ &= \frac{1}{2} \mathbb{E}_{p_{g_\theta}} \left[\log \frac{p_{g_\theta}}{p_{M_{\theta_0}}} \right] + \frac{1}{2} \mathbb{E}_{p_{g_\theta}} \left[\log \frac{p_{M_{\theta_0}}}{p_{M_\theta}} \right] \\ &+ \frac{1}{2} \mathbb{E}_{p_{data}} \left[\log \frac{p_{data}}{p_{M_{\theta_0}}} \right] + \frac{1}{2} \mathbb{E}_{p_{data}} \left[\log \frac{p_{M_{\theta_0}}}{p_{M_\theta}} \right] \\ &= \frac{1}{2} \mathbb{E}_{p_{g_\theta}} \left[\log \frac{p_{g_\theta}}{p_{M_{\theta_0}}} \right] + \frac{1}{2} \mathbb{E}_{p_{data}} \left[\log \frac{p_{data}}{p_{M_{\theta_0}}} \right] + \mathbb{E}_{p_{M_\theta}} \left[\log \frac{p_{M_{\theta_0}}}{p_{M_\theta}} \right] \\ &= \frac{1}{2} \text{KL}(p_{g_\theta} \| p_{M_{\theta_0}}) + \frac{1}{2} \text{KL}(p_{data} \| p_{M_{\theta_0}}) - \text{KL}(p_{M_\theta} \| p_{M_{\theta_0}}).\end{aligned}\quad (29)$$

Note that

$$\nabla_\theta \text{KL}(p_{M_\theta} \| p_{M_{\theta_0}}) |_{\theta=\theta_0} = 0. \quad (30)$$

Taking derivatives of Eq.(28) w.r.t θ at θ_0 we get

$$\begin{aligned}\nabla_\theta \mathbb{E}_{p(y)} [\text{KL}(p_\theta(\mathbf{x}|y) \| p_{\theta_0}(\mathbf{x}))] |_{\theta=\theta_0} &= \\ &= \nabla_\theta \left(\frac{1}{2} \text{KL}(p_{g_\theta} \| p_{M_{\theta_0}}) |_{\theta=\theta_0} + \frac{1}{2} \text{KL}(p_{data} \| p_{M_{\theta_0}}) \right) |_{\theta=\theta_0} \\ &= \nabla_\theta \text{JSD}(p_{g_\theta} \| p_{data}) |_{\theta=\theta_0}.\end{aligned}\quad (31)$$

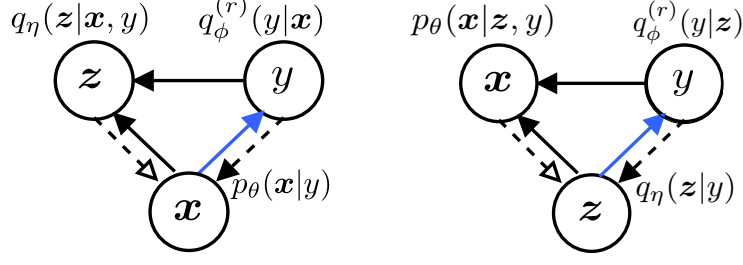


Figure 6: **Left:** Graphical model of InfoGAN. **Right:** Graphical model of Adversarial Autoencoder (AAE), which is obtained by swapping data x and code z in InfoGAN.

Taking derivatives of the both sides of Eq.(26) at w.r.t θ at θ_0 and plugging the last equation of Eq.(31), we obtain the desired results. \square

C AAE/PM/CycleGAN

Adversarial Autoencoder (AAE) [35] can be obtained by swapping code variable z and data variable x of InfoGAN in the graphical model, as shown in Figure 6. To see this, we directly write down the objectives represented by the graphical model in the right panel, and show they are precisely the original AAE objectives proposed in [35]. We present detailed derivations, which also serve as an example for how one can translate a graphical model representation to the mathematical formulations. Readers can do similarly on graphical models of GANs, InfoGANs, VAEs, and many other relevant variants and write down the respective objectives conveniently.

We stick to the notational convention in the paper that parameter θ is associated with the distribution over x , parameter η with the distribution over z , and parameter ϕ with the distribution over y . Besides, we use p to denote the distributions over x , and q the distributions over z and y .

From the graphical model, the inference process (dashed-line arrows) involves implicit distribution $q_\eta(z|y)$ (where x is encapsulated). As in the formulations of GANs (Eq.4 in the paper) and VAEs (Eq.13 in the paper), $y = 1$ indicates the real distribution we want to approximate and $y = 0$ indicates the approximate distribution with parameters to learn. So we have

$$q_\eta(z|y) = \begin{cases} q_\eta(z|y=0) & y = 0 \\ q(z) & y = 1, \end{cases} \quad (32)$$

where, as z is the hidden code, $q(z)$ is the prior distribution over z ¹, and the space of x is degenerated. Here $q_\eta(z|y=0)$ is the implicit distribution such that

$$z \sim q_\eta(z|y=0) \iff z = E_\eta(x), \quad x \sim p_{data}(x), \quad (33)$$

where $E_\eta(x)$ is a deterministic transformation parameterized with η that maps data x to code z . Note that as x is a visible variable, the pre-fixed distribution of x is the empirical data distribution.

On the other hand, the generative process (solid-line arrows) involves $p_\theta(x|z, y)q_\phi^{(r)}(y|z)$ (here $q^{(r)}$ means we will swap between q^r and q). As the space of x is degenerated given $y = 1$, thus $p_\theta(x|z, y)$ is fixed without parameters to learn, and θ is only associated to $y = 0$.

With the above components, we maximize the log likelihood of the generative distributions $\log p_\theta(x|z, y)q_\phi^{(r)}(y|z)$ conditioning on the variable z inferred by $q_\eta(z|y)$. Adding the prior distributions, the objectives are then written as

$$\begin{aligned} \max_\phi \mathcal{L}_\phi &= \mathbb{E}_{q_\eta(z|y)p(y)} [\log p_\theta(x|z, y)q_\phi(y|z)] \\ \max_{\theta, \eta} \mathcal{L}_{\theta, \eta} &= \mathbb{E}_{q_\eta(z|y)p(y)} [\log p_\theta(x|z, y)q_\phi^{(r)}(y|z)]. \end{aligned} \quad (34)$$

¹See section 6 of the paper for the detailed discussion on prior distributions of hidden variables and empirical distribution of visible variables

Again, the only difference between the objectives of ϕ and $\{\theta, \eta\}$ is swapping between $q_\phi(y|z)$ and its reverse $q_\phi^r(y|z)$.

To make it clearer that Eq.(34) is indeed the original AAE proposed in [35], we transform \mathcal{L}_ϕ as

$$\begin{aligned} \max_\phi \mathcal{L}_\phi &= \mathbb{E}_{q_\eta(z|y)p(y)} [\log q_\phi(y|z)] \\ &= \frac{1}{2} \mathbb{E}_{q_\eta(z|y=0)} [\log q_\phi(y=0|z)] + \frac{1}{2} \mathbb{E}_{q_\eta(z|y=1)} [\log q_\phi(y=1|z)] \\ &= \frac{1}{2} \mathbb{E}_{z=E_\eta(x), x \sim p_{data}(x)} [\log q_\phi(y=0|z)] + \frac{1}{2} \mathbb{E}_{z \sim q(z)} [\log q_\phi(y=1|z)]. \end{aligned} \quad (35)$$

That is, the discriminator with parameters ϕ is trained to maximize the accuracy of distinguishing the hidden code either sampled from the true prior $p(z)$ or inferred from observed data example x . The objective $\mathcal{L}_{\theta, \eta}$ optimizes θ and η to minimize the reconstruction loss of observed data x and at the same time to generate code z that fools the discriminator. We thus get the conventional view of the AAE model.

Predictability Minimization (PM) [51] is the early form of adversarial approach which aims at learning code z from data such that each unit of the code is hard to predict by the accompanying code predictor based on remaining code units. AAE closely resembles PM by seeing the discriminator as a special form of the code predictors.

CycleGAN [57] is the model that learns to translate examples of one domain (e.g., images of horse) to another domain (e.g., images of zebra) and vice versa based on unpaired data. Let x and z be the variables of the two domains, then the objectives of AAE (Eq.34) is precisely the objectives that train the model to translate x into z . The reversed translation is trained with the objectives of InfoGAN (Eq.9 in the paper), the symmetric counterpart of AAE.

D Proof of Lemme 2

Proof. For the reconstruction term:

$$\begin{aligned} &\mathbb{E}_{p_{\theta_0}(x)} [\mathbb{E}_{q_\eta(z|x, y) q_\eta^r(y|x)} [\log p_\theta(x|z, y)]] \\ &= \frac{1}{2} \mathbb{E}_{p_{\theta_0}(x|y=1)} [\mathbb{E}_{q_\eta(z|x, y=0), y=0 \sim q_\eta^r(y|x)} [\log p_\theta(x|z, y=0)]] \\ &\quad + \frac{1}{2} \mathbb{E}_{p_{\theta_0}(x|y=0)} [\mathbb{E}_{q_\eta(z|x, y=1), y=1 \sim q_\eta^r(y|x)} [\log p_\theta(x|z, y=1)]] \\ &= \frac{1}{2} \mathbb{E}_{p_{data}(x)} [\mathbb{E}_{\tilde{q}_\eta(z|x)} [\log \tilde{p}_\theta(x|z)]] + const, \end{aligned} \quad (36)$$

where $y = 0 \sim q_\eta^r(y|x)$ means $q_\eta^r(y|x)$ predicts $y = 0$ with probability 1. Note that both $q_\eta(z|x, y = 1)$ and $p_\theta(x|z, y = 1)$ are constant distributions without free parameters to learn; $q_\eta(z|x, y = 0) = \tilde{q}_\eta(z|x)$, and $p_\theta(x|z, y = 0) = \tilde{p}_\theta(x|z)$.

For the KL prior regularization term:

$$\begin{aligned} &\mathbb{E}_{p_{\theta_0}(x)} [\text{KL}(q_\eta(z|x, y) q_\eta^r(y|x) \| p(z|y)p(y))] \\ &= \mathbb{E}_{p_{\theta_0}(x)} \left[\int q_\eta^r(y|x) \text{KL}(q_\eta(z|x, y) \| p(z|y)) dy + \text{KL}(q_\eta^r(y|x) \| p(y)) \right] \\ &= \frac{1}{2} \mathbb{E}_{p_{\theta_0}(x|y=1)} [\text{KL}(q_\eta(z|x, y=0) \| p(z|y=0)) + const] + \frac{1}{2} \mathbb{E}_{p_{\theta_0}(x|y=1)} [const] \\ &= \frac{1}{2} \mathbb{E}_{p_{data}(x)} [\text{KL}(\tilde{q}_\eta(z|x) \| \tilde{p}(z))]. \end{aligned} \quad (37)$$

Combining Eq.(36) and Eq.(37) we recover the conventional VAE objective in Eq.(7) in the paper. \square

E Importance Weighted GANs (IWGAN)

From Eq.(4) in the paper, we can view GANs as maximizing a lower bound of the “marginal log-likelihood”:

$$\begin{aligned}\log q(y) &= \log \int p_\theta(\mathbf{x}|y) \frac{q^r(y|\mathbf{x})p_{\theta_0}(\mathbf{x})}{p_\theta(\mathbf{x}|y)} d\mathbf{x} \\ &\geq \int p_\theta(\mathbf{x}|y) \log \frac{q^r(y|\mathbf{x})p_{\theta_0}(\mathbf{x})}{p_\theta(\mathbf{x}|y)} d\mathbf{x} \\ &= -\text{KL}(p_\theta(\mathbf{x}|y) \| q^r(\mathbf{x}|y)) + \text{const.}\end{aligned}\quad (38)$$

We can apply the same importance weighting method as in IWAE [5] to derive a tighter bound.

$$\begin{aligned}\log q(y) &= \log \mathbb{E} \left[\frac{1}{k} \sum_{i=1}^k \frac{q^r(y|\mathbf{x}_i)p_{\theta_0}(\mathbf{x}_i)}{p_\theta(\mathbf{x}_i|y)} \right] \\ &\geq \mathbb{E} \left[\log \frac{1}{k} \sum_{i=1}^k \frac{q^r(y|\mathbf{x}_i)p_{\theta_0}(\mathbf{x}_i)}{p_\theta(\mathbf{x}_i|y)} \right] \\ &= \mathbb{E} \left[\log \frac{1}{k} \sum_{i=1}^k w_i \right] \\ &:= \mathcal{L}_k(y)\end{aligned}\quad (39)$$

where we have denoted $w_i = \frac{q^r(y|\mathbf{x}_i)p_{\theta_0}(\mathbf{x}_i)}{p_\theta(\mathbf{x}_i|y)}$. We recover the lower bound of Eq.(38) when setting $k = 1$.

To maximize the importance weighted lower bound, we compute the gradient:

$$\begin{aligned}\nabla_\theta \mathcal{L}_k(y) &= \nabla_\theta \mathbb{E}_{\mathbf{z}_1, \dots, \mathbf{z}_k} \left[\log \frac{1}{k} \sum_{i=1}^k w_i \right] = \mathbb{E}_{\mathbf{z}_1, \dots, \mathbf{z}_k} \left[\nabla_\theta \log \frac{1}{k} \sum_{i=1}^k w(y, \mathbf{x}(\mathbf{z}_i, \boldsymbol{\theta})) \right] \\ &= \mathbb{E}_{\mathbf{z}_1, \dots, \mathbf{z}_k} \left[\sum_{i=1}^k \widetilde{w}_i \nabla_\theta \log w(y, \mathbf{x}(\mathbf{z}_i, \boldsymbol{\theta})) \right],\end{aligned}\quad (40)$$

where $\widetilde{w}_i = w_i / \sum_{i=1}^k w_i$ are the normalized importance weights. We expand the weight at $\boldsymbol{\theta} = \boldsymbol{\theta}_0$

$$w_i|_{\boldsymbol{\theta}=\boldsymbol{\theta}_0} = \frac{q^r(y|\mathbf{x}_i)p_{\theta_0}(\mathbf{x}_i)}{p_\theta(\mathbf{x}_i|y)} = q^r(y|\mathbf{x}_i) \frac{\frac{1}{2}p_{\theta_0}(\mathbf{x}_i|y=0) + \frac{1}{2}p_{\theta_0}(\mathbf{x}_i|y=1)}{p_{\theta_0}(\mathbf{x}_i|y)} \Big|_{\boldsymbol{\theta}=\boldsymbol{\theta}_0}. \quad (41)$$

The ratio of $p_{\theta_0}(\mathbf{x}_i|y=0)$ and $p_{\theta_0}(\mathbf{x}_i|y=1)$ is intractable. Using the Bayes’ rule and approximating with the discriminator distribution, we have

$$\frac{p(\mathbf{x}|y=0)}{p(\mathbf{x}|y=1)} = \frac{p(y=0|\mathbf{x})p(y=1)}{p(y=1|\mathbf{x})p(y=0)} \approx \frac{q(y=0|\mathbf{x})}{q(y=1|\mathbf{x})}. \quad (42)$$

Plug Eq.(42) into the above we have

$$w_i|_{\boldsymbol{\theta}=\boldsymbol{\theta}_0} \approx \frac{q^r(y|\mathbf{x}_i)}{q(y|\mathbf{x}_i)}. \quad (43)$$

In Eq.(40), the derivative $\nabla_\theta \log w_i$ is

$$\nabla_\theta \log w(y, \mathbf{x}(\mathbf{z}_i, \boldsymbol{\theta})) = \nabla_\theta \log q^r(y|\mathbf{x}(\mathbf{z}_i, \boldsymbol{\theta})) + \nabla_\theta \log \frac{p_{\theta_0}(\mathbf{x}_i)}{p_\theta(\mathbf{x}_i|y)}. \quad (44)$$

Similar to GAN, we omit the second term on the RHS of the equation. Therefore, the resulting update rule of $p_\theta(\mathbf{x}|y)$ is

$$\nabla_\theta \mathcal{L}_k(y) = \mathbb{E}_{\mathbf{z}_1, \dots, \mathbf{z}_k} \left[\sum_{i=1}^k \widetilde{w}_i \nabla_\theta \log q^r(y|\mathbf{x}(\mathbf{z}_i, \boldsymbol{\theta})) \right] \quad (45)$$

F Experimental Results of SVAE

Table 3 shows the results.

	1%	10%
SVAE	0.9412 \pm .0039	0.9768 \pm .0009
AASVAE	0.9425\pm.0045	0.9797\pm.0010

Table 3: Classification accuracy of semi-supervised VAEs and the adversary activated extension on the MNIST test set, with varying size of real labeled training examples.